PHYSICSAccess Research Paper
ISSN Online: 2756-3898, ISSN Print: 2714-500X https://doi.org/10.47514/phyaccess.sp.iss.2022.1.002

Influence of Front Contact Layer on the Performance of Bismuth-Based Perovskite Solar Cells

Faruk Sani[1] and Sanusi Abdullahi[1]

[1] Department of Physics, Usmanu Danfodiyo University, Sokoto, Sokoto State, Nigeria.

Corresponding E-mail: faruk.sani@udusok.edu.ng

Received 30-09-2022
Accepted for publication 27-10-2022
Published 08-11-2022

Abstract

Numerical analysis has been carried out using SCAPS-1D to investigate the power conversion efficiency of bismuth-based perovskite solar cells employing various Transparent Conductive Oxides (TCOs) such as Molybdenum Trioxide (MoO_3), Boron-doped Zinc Oxide (BZO) and Zinc Oxide (ZnO). For the initial simulation, the power conversion efficiencies obtained for MoO_3, BZO and ZnO were 0.24 %, 0.17 % and 0.17 % respectively. The influence of thickness, donor concentration and working temperature of the TCOs were varied to study their impact on the device's photovoltaic performance. By varying the thickness, doping concentration and operating temperature, the electrical parameters observed for the three selected TCOs exhibited insignificant impact on the device's performance. However, the highest performance was achieved using MoO_3 at the thickness of 200 nm, donor concentration of $1 \times 10^{17}\ cm^{-3}$and the operating temperature of 300 K with the corresponding power conversion efficiency of 0.24 %, Jsc, Voc and FF of 0.2610 mA/cm^2, 1.6509 V and 54.97 % respectively. The numerical simulation shows the potential of designing and fabricating an improved bismuth-based perovskite solar cell with MoO_3 as front contact as an alternative to Fluorine-doped Tin Oxide (FTO) and Indium-doped Tin Oxide (ITO).

Keywords: Bismuth; donor concentration; efficiency; molybdenum trioxide; perovskite

I. Introduction

Perovskite – based solar cells have shown an excellent performance due to their exceptional properties such as high absorption coefficient, high charge carrier mobility, low surface recombination rate, long diffusion length, direct and tunable band gap and relatively simple methods of processing [1 - 3]. The efficiency of these promising materials has rapidly increased from 3.8 % in 2009 [4] to 26.1 % in 2022 [5]. Transparent conductive oxides (TCOs) have been commonly used as a front contact in perovskite-based solar cells. These TCOs are optically transparent and electrically conductive materials. For a TCO to work efficiently, its band gap must be greater than or equal to 3.1 eV [6]. The TCO having high band gap transmits about 80 % of visible light [7 - 9]. The most commonly used TCOs are indium-doped tin oxide (ITO) and fluorine-doped tin oxide (FTO) owing to their high transparency and low resistivity [10 -17]. Though, indium metal is reported as rare, toxic material, expensive and environmentally-unfriendly [18-21]. Moreover, the low electrical conductivity, high leakage current and rigid to patterning by wet etching are the major drawbacks associated with FTO as reported by [22].

To further discover an alternative TCO, this work has designed and simulated a bismuth-based perovskite solar cell to investigate the influence of Molybdenum trioxide (MoO_3),

boron-doped and Zinc Oxide (ZnO) used as front contact using SCAPS-1D. To attain the optimal device performance, the thickness, defect density, donor density and operating temperature of the TCOs were also studied for the three different TCOs. The device structure is presented in Fig. 1.

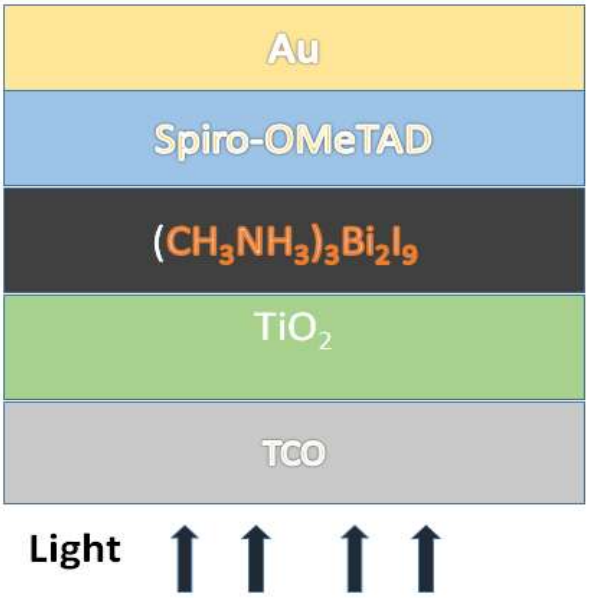

Fig. 1 The device structure of the bismuth-based perovskite solar cells.

II. Materials and Numerical Method

A. Materials

The materials used are methyl-ammonium bismuth iodide (MBI) used as the absorber layer, TiO_2 served as electron transporting layer (ETL), Spiro-OMeTAD used as hole transporting layer (HTL). The proposed TCOs are MoO_3, BZO and ZnO acted as front contact while Gold (Au) as a counter electrode. The simulation input parameters of these layers were obtained from previous literature [23 – 36] and were summarized in Table I.

Table I Input values for simulation of $(CH_3NH_3)_3Bi_2I_9$ [23 – 36]

Parameters	MoO_3	ZnO	BZO	TiO_2	$(CH_3NH_3)_3Bi_2I_9$	Spiro-OMeTAD
Thickness (nm)	200 (varied)	200 (varied)	200 (varied)	100	100	200
E_g (eV)	3.8	3.3	3.3	3.2	3.2	3.0
X (eV)	4.1	4.6	4.55	3.9	4.26	2.45
ε_r	9	9	9	9.0	100	3.0
N_c (cm^{-3})	2.2×10^{18}	4×10^{18}	3×10^{18}	1×10^{21}	2×10^{18}	1×10^{19}
N_v (cm^{-3})	1.8×10^{19}	2×10^{19}	1.8×10^{19}	2×10^{20}	1.8×10^{19}	1×10^{19}
μ_n (cm^2/Vs)	30	100	100	20	4	0.0002
μ_p (cm^2/Vs)	6	25	31	10	2	0.0002
N_d (cm^{-3})	1×10^{17} (varied)	1×10^{17} (varied)	10^{20} (varied)	1×10^{19}	1×10^{18}	0
N_a (cm^{-3})	0	0	0	0	0	1×10^{18}
N_t (cm^{-3})	1×10^{14}	1×10^{14}	1×10^{14}	1×10^{15}	2.5×10^{14}	1×10^{15}

B. Numerical Method

In this study, the design and simulation were conducted using SCAPS-1D (SCAPS 3.3.10 version) simulating software with adopted AM1.5G solar illumination, incident power density of 1000 W/cm2, work point bias 0 V, frequency of $1.0 \times 10^6\ Hz$, electron and hole thermal velocities $10^7\ cm^{-1}$ and the input parameters itemized in Table I. The SCAPS-1D was designed and developed by the Department of Electronics and Information Systems (ELIS), University of Gent, Belgium [38]. This simulating software can compute J-V characteristics of the perovskite solar cells by solving the Poisson equations, continuity equations for electrons and holes, and carrier transport [38, 39]. The simulation step by step procedure is shown in Fig. 2.

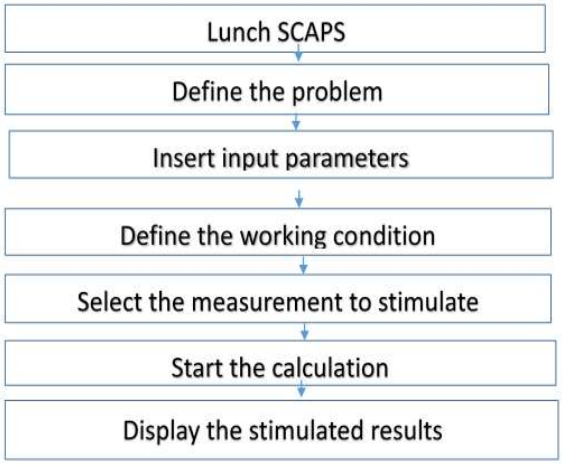

Fig. 2 SCAPS step by step procedure.

III. Results and Discussion

A. Effect of TCO on the $(CH_3NH_3)_3Bi_2I_9$ PSC

A transparent conducive oxide layer plays a significant role in the performance of a solar cell since it is used as a front contact [41]. Fig. 3 displays the simulated J-V characteristics of the devices with the various TCOs (MoO_3, ZnO, and BZO). The photovoltaic parameters obtained were presented in Table II. From Table II, it can be observed that the device with the MoO_3 exhibits the highest PCE while the devices with the ZnO and BZO acquire the same PCE. This shows that doping ZnO with boron metal might not increase the electrical conductivity of the TCO which is in line with the findings of [38]. This is because boron atom acts as electron donor in ZnO, increasing the electrical conductivity and decreasing the transparency, hence, this decrease in transparency renders the electrical conductivity insignificant. The highest PCE was achieved using MoO_3 with photovoltaic parameters; 1.6509 V, 0.2610mA/cm^2, 54.97 % and 0.24 % for Voc, Jsc, FF, and PCE respectively. This indicates that high band-gap enables the transparent conductive oxide to transmit 80 % or more of visible light which has also been reported by [7 -9]. The results obtained also show that MoO_3 has high ability in transmitting

light into the device than the doped and undoped-zinc oxide.

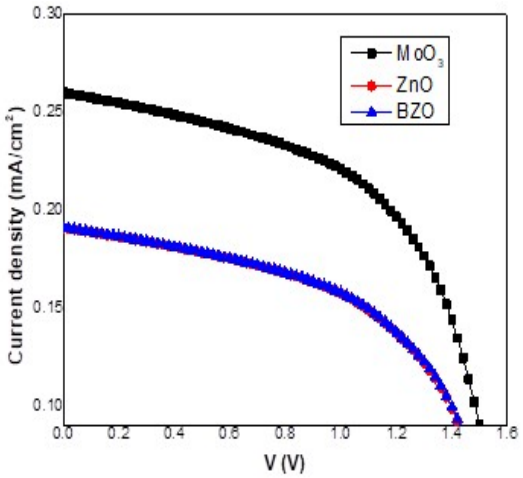

Fig. 3 Influence of the three different TCOs on the J-V characteristics

Table II Photovoltaic parameters obtained using MoO_3, BZO and ZnO as front contact.

Parameters	MoO_3	ZnO	BZO
V_{oc} (V)	1.6509	1.6511	1.6514
J_{sc} (mA/cm^2)	0.2610	0.1911	0.1913
FF (%)	54.97	52.36	52.52
PCE (%)	0.24	0.17	0.17

B. Effect of TCO thickness on the performance MBI Perovskite solar cells

The influence of TCO layer thickness was investigated using the numerical simulation. The thickness was varied from 300 nm to 1200 nm for each of the chosen TCO and the remaining input parameters kept constant. Fig. 4 show the plotted J-V curves obtained for MoO_3, BZO and ZnO based devices. Similarly, the photovoltaic parameters obtained for MoO_3, BZO and ZnO were tabulated in Table III, IV and V respectively. As shown in the Table III, the Voc is relatively unchanged in contrast to Jsc and FF which slightly decreased from $0.2586\ mA/cm^2 - 0.2505\ mA/cm^2$ and $54.9\ 2\% - 54.65\ \%$ respectively. This shows that the decrease in Jsc might be responsible for the decrease in FF as reported by [40]. On the other hand, no any significant change in PCE was observed. From Tables IV and V, rapid decrease in Jsc and FF was observed as the thicknesses of ZnO and BZO increased. Generally, the increase in TCO thickness results in increased optical absorption which can prolong the path of light and cause internal scattering as reported by [39]. Hence, this decreases the quantity of photons being absorbed by the perovskite absorber layer and consequently the power conversion efficiency decreases.

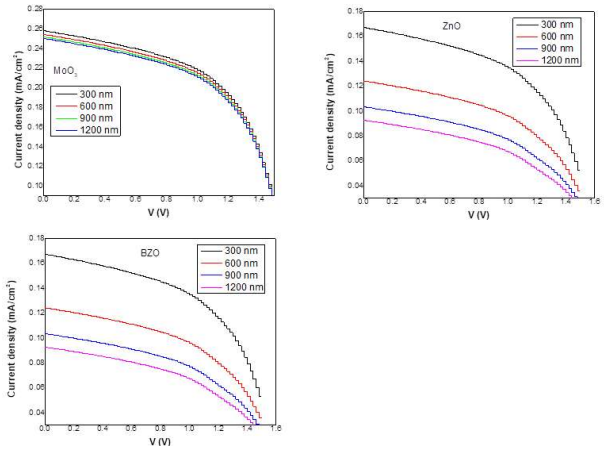

Fig. 4 Effect of TCOs thickness on the J-V characteristics of the device.

Table III Photovoltaic parameters for MoO_3 at different thickness

Thickness (nm)	V_{oc} (V)	J_{sc} (mA/cm^2)	FF (%)	PCE (%)
300	1.6509	0.2585	54.92	0.23
600	1.6509	0.2547	54.80	0.23
900	1.6509	0.2522	54.71	0.23
1200	1.6509	0.2505	54.65	0.23

Table IV Photovoltaic parameters for ZnO at different thickness

Thickness (nm)	V_{oc} (V)	J_{sc} (mA/cm^2)	FF (%)	PCE (%)
300	1.6515	0.1675	51.17	0.14
600	1.6527	0.1245	48.15	0.10
900	1.6535	0.1037	46.05	0.08
1200	1.6538	0.0929	44.69	0.07

Table V Photovoltaic parameters for BZO at different thickness

Thickness (nm)	V_{oc} (V)	J_{sc} (mA/cm^2)	FF (%)	PCE (%)
300	1.6514	0.1676	51.31	0.14
600	1.6513	0.1245	48.25	0.10
900	1.6511	0.1037	46.13	0.08
1200	1.6508	0.0929	44.76	0.07

C. Effect of TCO doping concentration on the performance MBI Perovskite solar cells

The doping concentrations of the TCOs were varied from $1.0 \times 10^{14}\ cm^{-3}$ to $1.0 \times 10^{20}\ cm^{-3}$ while the remaining input parameters kept constant. Fig. 5 show the J-V curves obtained using the three different TCOs. It could be seen from Tables VI, VII and VIII, all the photovoltaic parameters obtained remain constant as the doping concentration

increased. This shows that deep and shallow donors cannot contribute to n-type conductivity due to presence of oxygen as revealed by [42].

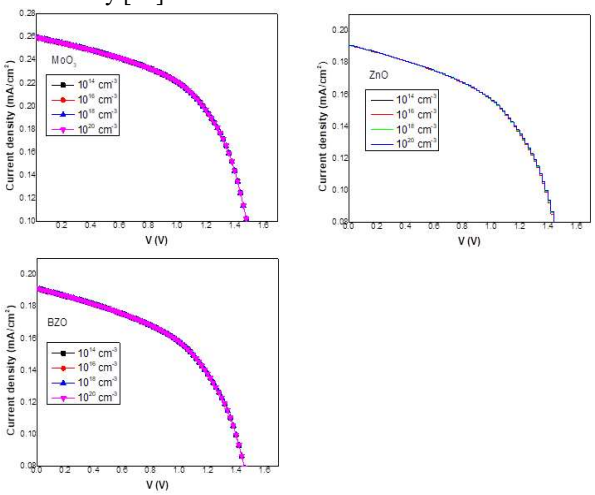

Fig. 5 Effect of TCOs doping concentration on the J-V characteristics

Table VI Photovoltaic parameters for MoO_3 with different donor concentration

Doping Concentration (cm^{-3})	V_{oc} (V)	J_{sc} (mA/cm^2)	FF (%)	PCE (%)
10^{14}	1.6509	0.2601	54.97	0.24
10^{16}	1.6509	0.2601	54.97	0.24
10^{18}	1.6509	0.2601	54.97	0.24
10^{20}	1.6509	0.2601	54.97	0.24

Table VII Photovoltaic parameters for ZnO with different donor concentration

Doping Concentration (cm^{-3})	V_{oc} (V)	J_{sc} (mA/cm^2)	FF (%)	PCE (%)
10^{14}	1.6505	0.1911	52.35	0.17
10^{16}	1.6505	0.1911	52.35	0.17
10^{18}	1.6535	0.1912	52.39	0.17
10^{20}	1.6541	0.1913	52.45	0.17

Table VIII Photovoltaic parameters for BZO with different donor concentration

Doping Concentration (cm^{-3})	V_{oc} (V)	J_{sc} (mA/cm^2)	FF (%)	PCE (%)
10^{14}	1.6506	0.1912	52.50	0.17
10^{16}	1.6507	0.1912	52.50	0.17
10^{18}	1.6515	0.1913	52.50	0.17
10^{20}	1.6514	0.1913	52.52	0.17

D. Effect of working temperature

Influence of working temperature on the device performance was studied using the three different TCOs, the operating temperature was varied from 350 K to 500 K while the remaining input values remain constant. Fig. 6 presents the J-V characteristics of the devices. The parameters obtained are tabulated in Tables IX, X and XI. It can be seen from Tables IX, X and XI that there is increase in Voc and decrease in Jsc and FF while the power conversion efficiencies remain steady as the operating temperature increases. Generally, the working temperature has less effect on the cell performance.

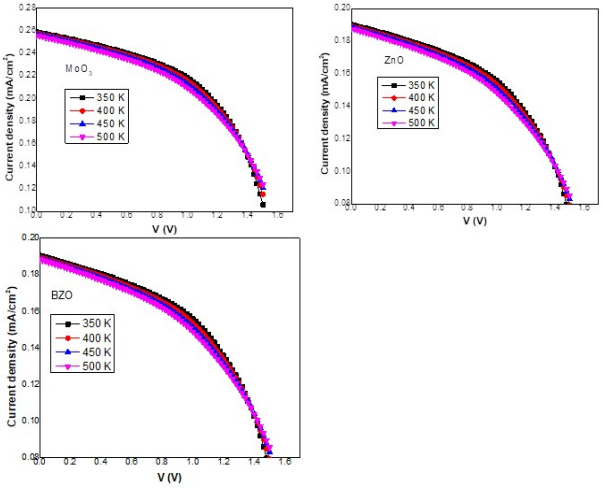

Fig. 6 Effect of TCOs working temperature on the J-V characteristics

Table IX Influence of temperature on the device using MoO_3

Parameters	350 K	400 K	450 K	500 K
V_{oc} (V)	1.7194	1.7913	1.8619	1.9289
J_{sc} (mA/cm^2)	0.2589	0.2578	0.2567	0.2556
FF (%)	52.28	49.70	47.31	45.14
PCE (%)	0.23	0.23	0.23	0.23

Table X Influence of temperature on the device using ZnO

Parameters	350 K	400 K	450 K	500 K
V_{oc} (V)	1.7188	1.7898	1.8592	1.9247
J_{sc} (mA/cm^2)	0.1903	0.1893	0.1885	0.1876
FF (%)	49.88	47.35	45.01	42.92
PCE (%)	0.16	0.16	0.16	0.15

Table XI Influence of temperature on the device using BZO

Parameters	350 K	400 K	450 K	500 K
V_{oc} (V)	1.7189	1.7898	1.8593	1.9250
J_{sc} (mA/cm^2)	0.1904	0.1894	0.1887	0.1882
FF (%)	49.88	47.36	45.02	42.96
PCE (%)	0.16	0.16	0.16	0.16

IV. CONCLUSION

In this work, $(CH_3NH_3)_3Bi_2I_9$ perovskite solar cells employing three different TCOs (MoO_3, ZnO, and BZO) were studied using SCAPS Simulating software. The device performances were also studied against varied TCO thickness,

doping concentration and working temperature. The results show that controlling the thickness of the TCOs is the most important factor in enhancing the efficiency of the perovskite-based solar cells. However, MoO_3 exhibited optimum efficiency of 0.24 % in contrast to ZnO and BZO with efficiency of 0.17 % each. It can be concluded that MoO_3 is a possible alternative to FTO and ITO as a front contact layer in perovskite solar cells.

ACKNOWLEDGMENT

The authors would like to thank Dr. Marc Burgelman and his staff of Department of Electronics and Information System, University of Gent for programming and distribution of the SCAPS simulation software.

CONFLICTS OF INTEREST

The authors declare no conflict of interest.

References

[1] Q. Chen, N. D. Marco, Y. Yang, T. B. Song, C. C. Chen, H. Zhou and Y. Yang, "Under the Spotlight: The Organic-Inorganic Hybrid Halide Perovskite for Optoelctronic Applications", Nano Today, vol. 10, pp. 355-396, 2015.

[2] M. A. Green, A. Ho-Baillie, and H. J. Snaith, "The emergence of perovskite solar cells". Nat. Photonics, vol. 8, no. 7, pp. 506–514, 2014.

[3] S. Srivastava, A. K. Singh, P. Kumar and B. Pradhan, "Comparative Performance Analysis of Lead-Free Perovskite Cells by Numerical Simulation", Res. Sq., 2021.

[4] A. Kojima, K. Teshima, Y. Shirai, and T. Miyasaka, "Organometal Halide Perovskites as Visible- Light Sensitizers for Photovoltaic Cells", J. of Amer. Chem. Soc., 131, 6050–6051. 2009.

[5] NREL, 2022. [Online]. Available: https://www.nrel.gov/pv/cell-efficiency.html Accessed on: August, 21, 2022.

[6] C. Guillén and J. Herrero, "TCO/metal/TCO structures for energy and flexible Electronics", Thin Solid Films, vol. 520, pp. 1–17, 2011.

[7] S. M. Bawaked, S. Sathasivam, D.S. Bhachu, N. Chadwick, A.Y. Obaid, S. Al-Thabaiti, S. N. Basahel, C. J. Carmalt, and I. P. Parkin, "Aerosol assisted chemical vapor deposition of conductive and photocatalytically active tantalum doped titanium dioxide films", J. Mater. Chem., vol. A 2, pp. 12849, 2014.

[8] D. S. Bhachu, G. Sankar, I.P. Parkin, "Aerosol assisted chemical vapor deposition of transparent conductive zinc oxide films", Chem. Mater., vol. 24, pp. 4704–4710. 2012.

[9] S. Sathasivam, D. S. Bhachu, Y. Lu, N. Chadwick, S. A. Althabaiti, A. O. Alyoubi, S. N. Basahel,, C. J. Carmalt, and I. P. Parkin, "Tungsten doped TiO_2 with enhanced photocatalytic and optoelectrical properties via aerosol assisted chemical vapor deposition", Sci. Rep. 2015.

[10] N. K. Noel, S. D. Stranks, A. Abate, C. Wehrenfennig, S. Guarnera, A.-A. Sadhanala, A. Haghighirad, G. E. Eperon, S. K. Pathak, and M. B. Johnston, "Lead-free organic– inorganic tin halide perovskites for photovoltaic applications, Eng. Environ. Sci., vol. 7, pp. 3061–3068, 2014.

[11] F. Hao, C.C. Stoumpos, D.H. Cao, R.P. Chang, and M.G. Kanatzidis, "Lead-free solid- state organic–inorganic halide perovskite solar cells", Nat. Photonics, vol. 8, pp. 489, 2014.

[12] F. Hao, C. C. Stoumpos, P. Guo, N. Zhou, T. J. Marks, R. P. Chang, and M. G. Kanatzidis, "Solvent-mediated crystallization of $CH_3NH_3SnI_3$ films for heterojunction depleted perovskite solar cells", J. Amer. Chem. Soc., vol. 137, pp. 11445–11452, 2015.

[13] T. Yokoyama, D. H. Cao, C. C. Stoumpos, T.-B. Song, Y. Sato, S. Aramaki and M. G. Kanatzidis, "Overcoming short-circuit in lead-free $CH_3NH_3SnI_3$ perovskite solar cells via kinetically controlled gas–solid reaction film fabrication process", J. Phys. Chem. Lett., vol. 7, pp. 776–782. 2016.

[14] T. Fujihara, S. Terakawa, T. Matsushima, C. Qin, M. Yahiro, and C. Adachi, " Fabrication of high coverage MASnI3 perovskite films for stable, planar heterojunction solar cells", J. Mater. Chem. C., vol. 5, pp. 1121–1127, 2017.

[15] Y. Yu, D. Zhao, C.R. Grice, W. Meng, C. Wang, W. Liao, A.J. Cimaroli, H. Zhang, K. Zhu, and Y. Yan, "Thermally evaporated methyl-ammonium tin triiodide thin films for lead-free perovskite solar cell fabrication", RSC Adv., vol. 6, pp. 90248–90254, 2016.

[16] L. Peng, and W. Xie, "Theoretical and experimental investigations on the bulk photovoltaic in lead-free perovskites MASnI3 and FASnI3", RSC Adv., vol. 10, pp. 14679–14688, 2020.

[17] D. A. Keller, H-N. Barad, E. Rosh-Hodesh, A. Zaban, and D. Cahen, "Can Fluorine-doped tin oxide, FTO, be more like indium-doped oxide, ITO? Reducing FTO Surface roughness by introducing additional SnO2 coating", Res. Lett., vol.8, no.3, pp. 1358-1362, 2018.

[18] H. Hagendorfer, K. Lienau, S. Nishiwaki, C. M. Fella, L. Kranz, A.R. Uhl, D. Jaeger, L. Luo, C. Gretener, S. Buecheler, Y.E. Romanyuk, A. N. Tiwari, "Highly transparent and conductive ZnO: Al thin films from a low temperature aqueous solution approach", Adv. Mater. 26, 632–636. 2014.

[19] T. Minami, "Transparent conducting oxide semiconductors for transparent Electrodes", Semicond. Sci. Technol., vol. 20, pp. S35–S44, 2005.

[20] M. Sibin ski, K. Znajdek, S. Walczak, M. Słoma, M. Górski, and A. Cenian, "Comparison of ZnO:Al, ITO and carbon nanotube transparent conductive layers in flexible solar cells applications",

Mater. Sci. Eng. B Solid-State Mater. Adv. Tech., vol. 177, pp. 1292–1298, 2012.
[21] S. Sohn, and H. Kim, "Transparent conductive oxide (TCO) films for organic light emissive devices (OLEDs)", Mater. Process Dev., pp. 233–274, 2011.
[22] H. Liu, V. Avrutin, N. Izyumskaya, Ü. Özgr, H. Morkoc, "Transparent conducting oxides for electrode applications in light emitting and absorbing devices", Superlatt. Microstruct., vol. 48, pp. 458–484, 2010.
[23] P. K. Patel, "Device simulation of highly efficient eco-friendly CH3NH3SnI3 perovskite solar cell". Scientific reports, vol. 11, pp. 3082, 2012.
[24] F. Baig, Y. H. Khattak, B. Marí, S. Beg, A. Ahmed, and K. Khan, "Efficiency Enhancement of $CH_3NH_3SnI_3$ Solar Cells by Device Modeling", J. of Elect. Mat., vol. 47, pp. 5275-5282, 2018.
[25] F. Azri, A. Meftah, N. Sengouga, and A. Meftah, "Electron and hole transport layers optimization by numerical simulation of a perovskite solar cell", Sol. Eng., vol. 181, pp. 372–378. 2019.
[26] T. Minemoto and M. Murata, "Impact of work function of back contact of perovskite solar cells without hole transport material analyzed by device simulation", Curr. Appl. Phys., vol. 14, pp. 1428–1433, 2014.
[27] R. Teimouri and R. Mohammadpour, "Potential application of $CuSbS_2$ as the hole transport material in perovskite solar cell: A simulation study", Superlattices Microstructure, vol. 118, pp. 116–122, 2018.
[28] A. Slami, M. Bouchaour, and L. Merad, "Comparative Study of Modelling of Perovskite Solar Cell with Different HTM Layers". Int. J. of Mat., vol. 7, 2020.
[29] F. Z. Bedia, A. Bedia, M. Aillerie, N. Maloufi, F. Genty, and B. Benyocef, "Influence of Al-doped ZnO transparent contacts deposited by a spray pyrolysis technique on performance of HIT solar cells", Eng. procedia, vol. 50, pp. 853-861, 2014.
[30] S. Raudik, A. M. Mozharov, D. M. Mitin, A. D. Bolshakov, P. M. Rajanna, A. G. Nasibulin, I. S. Mukhin, "Numerical simulation of the carbon nanotubes transport layer influence on performance of GaAs solar cells", IOP Conf. Series: J. of Phys., vol. 1124, no. 4, 2018.
[31] B. J. Baba, U. Mandapu, V. Vedanayakam, and K. Tyagarajan, "Optimization of high efficiency tin halide perovskite solar cells using SCAPS-1D". Int. J. of Sim. & Proc. Model., vol. 13, no. 3, pp. 221, 2018.
[32] M. A. Rahman, "Design and simulation of a high performance Cd-free Cu_2SnSe_3 solar cells with SnS electron-blocking hole transport layer and TiO_2 electron transport layer by SCAPS-1D". SN Appl. Sci., vol. 3, pp. 253, 2021.
[33] S. Ouedraogo, F. Zougmore, and J. M. Ndjaka, "Numerical analysis of copper-indium-Gallium-Diselinide-based solar cells by SCAPS-1D", Int. J. of Photoenergy, vol. 2, 2013.
[34] B. Zaid, M. S. Ulla, B. Hadjoudja and S. Gagui, "Role of TC films in improving the efficiency of Cds/MoS_2 heterojunction solar cells", J. of Nano and Elect. Phys., vol. 11, no. 2, 2019.
[35] B. Mozafari and S. Hoseini, "Using Molybdenum trioxide as a TCO layer to improve performance of CdTe/CdS thin film solar cell". Signal processing and Renewable Energy, pp. 57-65, 2020.
[36] O. U. Charles, "Investigation of Lead-free Bismuth Perovskite by Numerical Simulation using SCAPS", A thesis Presented to the Dept. of Mat. Sci. and Eng., Afric. Univ. of Sci. & Tech., Abuja, Nigeria. 2019.
[37] M. Burgelman, K. Decock, A. Niemegeers, J. Verschraegen, S. Degrave, "SCAPS Manual", Dept. of Elect. & Info. Sys. (ELIS), Univ. of Gent, Bel., 2012.
[38] H. Movla, "Optimization of the CIGS based thin film solar cells: numerical simulation and analysis", Optik, vol. 125, no. 1, pp. 67–70. 2014.
[39] A. Mohandes, M. Moradi, and H. Nadgaran, "Numerical Simulation of Inorganic $Cs_2AgBiBr_6$ as a Lead-free Perovskite using Device Simulation SCAPS-1D", Optical and Quantum Electronics, vol. 53, pp. 319, 2021
[40] E. D. Tareq, M. A. Samir and H. H. Waried, "Perovskite Solar Cells based on $CH_3NH_3SnI_3$ Structure, IOP Conf. series; Mat. Sci. and Eng., pp. 928, 2020.
[41] M. Joachim, R. Bernd, J. Springer, and M. Vanecek, "TCO and light trapping silicon thin film solar cells", Sci. Dir., vol. 77, pp. 917 – 930, 2004.
[42] A. Janotti and C. G. VandeWalle, "Fundamental of Zinc oxide as a semiconductor, Rep. Prog. Phys., vol. 72, 2009.